Available online at www.sciencedirect.com
SCIENCE DIRECT®
Acta Materialia 52 (2004) 285–292
Acta MATERIALIA
www.actamat-journals.com

Grain shape, grain boundary mobility and the Herring relation

A.E. Lobkovsky [a,*], A. Karma [a], M.I. Mendelev [b], M. Haataja [b], D.J. Srolovitz [b]

[a] Department of Physics, Northeastern University, Boston, MA 02115, USA
[b] Department of Mechanical & Aerospace Engineering, Princeton Materials Institute, Princeton University, Princeton, NJ 08544, USA

Received 27 June 2003; received in revised form 11 September 2003; accepted 12 September 2003

Abstract

Motivated by recent experiments on grain boundary migration in Al, we examine the question: does interface mobility depend on the nature of the driving force? We investigate this question in the Ising model and conclude that the answer is "no." This conclusion highlights the importance of including the second derivative of the interface energy with respect to inclination γ'' in the Herring relation in order to correctly describe the motion of grain boundaries driven by capillarity. The importance of this term can be traced to the entropic part of γ'', which can be highly anisotropic, such that the reduced mobility (i.e., the product of interface stiffness $\gamma + \gamma''$ and mobility) can be nearly isotropic even though the mobility itself is highly anisotropic. The cancellation of these two anisotropies (associated with stiffness and mobility) originates in the Ising model from the fact that the number of geometrically necessary kinks, and hence the kink configurational entropy, varies rapidly with inclination near low-energy/low mobility, but slowly near high-energy/high-mobility interfaces, where the kink density is high. This implies that *the stiffness is high where the mobility is low* and vice versa. Consequently, the grain shape can appear isotropic or highly anisotropic depending on whether its motion is driven by curvature or an external field, respectively, but the mobility itself is independent of driving force. We discuss the implications of these results for interpreting experimental observations and computer simulations of microstructural evolution, where γ'' is routinely neglected.

Keywords: Grian boundary migration; Interface driving force; Interface mobility; Monte Carlo simulation; Interface stiffness

1. Introduction

Most thermal processing strategies are designed to modify microstructure via physical processes that commonly involve interface motion (phase transformations, grain growth, etc.). Interface migration can occur in response to disparate driving forces, such as those associated with concentration gradients [1], stresses [2], and magnetic fields [3]. Typically, the driving force P is small, such that the net interface velocity v can be described by the simple linear relation

$$v = MP, \tag{1}$$

where M is the interface mobility.

Another important driving force for microstructure evolution is related to interface curvature, i.e., capillarity. This driving force differs from the ones discussed above in that it is associated with the interface itself, rather than external conditions or bulk thermodynamics. Herring [4] showed that this force is

$$P_\kappa = (\gamma + \gamma'')\kappa, \tag{2}$$

where κ is the interface curvature, γ is the interface free energy and γ'' is its second derivative with respect to interface inclination. Inserting the driving force from Eq. (2) into Eq. (1), we find

$$v = M(\gamma + \gamma'')\kappa = M^*\kappa, \tag{3}$$

where M^* is known as the reduced mobility, and the sum $\gamma + \gamma''$ as the interface stiffness. The importance of the stiffness is well-established for solidification where γ'' plays a crucial role in selecting both the orientation and the growth rate of dendrites [5]. The role of the stiffness in solid systems is comparatively less well understood. Experimentally determined interface free energies are only available in limited situations and interface stiffness

* Corresponding author. Tel.: +1-617-253-7278; fax: +1-617-253-1699.
E-mail address: leapfrog@neu.edu (A.E. Lobkovsky).

1359-6454/$30.00 © 2003 Acta Materialia Inc. Published by Elsevier Ltd. All rights reserved.
doi:10.1016/j.actamat.2003.09.012

data are rare. Because of this, the common practice has been to neglect the unknown γ'' and to approximate, without a real justification, Eq. (3) by

$$v = M\gamma\kappa. \tag{4}$$

The primary goal of the present work is to determine whether the approximation in Eq. (4) is reasonable or whether it can introduce important errors.

The mobility is usually considered to be independent of the driving force. The validity of this assertion is brought into question by some recent experiments [2] which investigated the migration of $\langle 111 \rangle$ tilt grain interfaces in high purity Al under the action of two distinct forces: an applied shear stress and capillarity. It was shown that migration under these two distinct driving forces were characterized by different values of the enthalpy of migration. On the basis of this observation, these authors [2] concluded that the mechanism of grain boundary migration was different under these different driving forces. This is a strong conclusion. The common assumption that interface mobility is independent of the source of the driving force is a fundamental tenet of the theory of the microstructure evolution. As such, this assumption and the apparent contradiction arising from the experimental results deserve careful attention.

Interface motion in the presence of two distinct driving forces was investigated within the framework of an Ising model on a triangular lattice [6]. This study demonstrated that while the interface free energy is only weakly anisotropic, the mobility of a nominally flat interface driven by an external field is strongly anisotropic at low temperature. However, no indication of anisotropy was observed when an initially circular grain shrank under the action of capillarity and with no applied field. Similarly, the shrinking of a half-loop grain yielded an interface profile which was consistent with the assumption of isotropy. On the other hand, when an external field which increases the shrinking rate was imposed, the interface profile exhibited a pronounced 6-fold symmetry consistent with that of the underlying lattice. The reason why the imposition of an isotropic applied field led to the development of an anisotropic profile remained unclear. The pronounced differences between interface profiles with and without an externally applied field led the authors [6] to speculate that interface mobility does indeed depend on the nature of the driving force. However, since the mobility of the curved interfaces always lied between the maximum and minimum of the anisotropic flat-interface mobilities, it was not possible to unambiguously conclude that interface mobility is not unique.

Of course, the Ising model is a rather crude model for interfaces in real materials. Yet, the fact that this model is so simple provides us with an ideal test bed for examining such fundamental questions as "is interface mobility unique?" Further, if we cannot understand the behavior of an interface in such a simple model, we have little hope of understanding it in real materials, where interface structure is much more complex and experiments are not as well controlled. Therefore, the main goal of our investigation is to determine whether the interface mobility depends on the nature of the driving force. Our negative answer to this question highlights the importance of including both the entropic part of γ and the second derivative term γ'' in Eqs. (2) and (3) in order to correctly describe curvature-driven interface motion. We explain why the inclusion the entropic part of γ'' resolves the apparent paradox that curvature-driven motion can be seemingly isotropic while the mobility is, in contrast, highly anisotropic. Furthermore, we argue that a similar answer should apply to real grain boundaries despite the fact that these interfaces are, admittedly, much more complex than the ones studied here.

2. Monte Carlo simulations

Let us consider the Ising model as a prototypical system with interfaces. The state of the system is described in terms of a set of spin values on each site of a lattice, $s_i = \pm 1$, where i labels lattice sites. Contiguous like spins are part of the same domain, while a domain wall separates nearest neighbor spins of opposite sign. The energy of the Ising model may be written in terms of the spatial distribution of spins and the two parameters J and H as

$$E = -\frac{J}{2}\sum_{\langle i,j \rangle} s_i s_j - H\sum_i s_i, \tag{5}$$

where the sum on i is over all N lattice sites in the system and the sum on $\langle i, j \rangle$ is over all nearest neighbor pairs of lattice sites. The interface energy in this model is proportional to J (> 0) and a non-zero value of H lowers the energy of one type of domain relative to the other. As such, H provides an external driving force for interface migration.

The evolution of the model was simulated using the Monte Carlo method with spin-flip dynamics (i.e., Glauber dynamics) [7]. In this approach, a site is chosen at random and an attempt is made to flip its sign (i.e., $s \to -s$). If the energy change, ΔE, is less than zero, this spin change is accepted. If $\Delta E \geqslant 0$, a random number R uniformly distributed on the domain $0 < R \leqslant 1$, is generated. If $R \leqslant \mathrm{e}^{-\Delta E/kT}$, this spin change is accepted; otherwise, the spin is returned to its original orientation. The present simulations were performed on a two-dimensional triangular lattice with lattice spacing a. Time, in these simulations, is proportional to the number of spin flip attempts. The time τ corresponds to N spin flip attempts.

The orientation dependence of the mobility was determined using Monte Carlo simulations with flat interfaces, in an applied field, H, using the simulation geometry shown in Fig. 1(a) (see [6] for details). We employed Mobius interface conditions in the x-direction, such that a flat interface can repeatedly traverse the simulation cell interface without perturbation (see [6]). Along the y-axis we employed a skew-periodic interface condition, such that the periodic images of the lattice are shifted from the original by L_y in the y-direction and by $L_y\tan\varphi$ in the x-direction (see Fig. 1(a)). The lattice orientation was chosen such that $\varphi = 0$ corresponds to the flat interface with the largest linear site density (see Fig. 1(b)). By analogy with the close-packed plane orientation in FCC lattice, we label this orientation [11]. The migration of this interface is well described by the classic kink theory which considers the rates of double kinks nucleation and kink propagation [6]. The mobility of the [11] flat interface exhibits an Arrhenius temperature dependence. The second limiting case is labeled [10] and is formed by rotating the interface by $\varphi = \pi/6$ from the [11] interface orientation (see Fig. 1(c)). The [10] interface moves athermally (i.e., the activation energy for migration is zero) and at low temperature moves with a much larger mobility than does the [11] interface. With increasing temperature, the mobilities of both interfaces approach the same value [6].

The orientation dependence of the flat interface mobility at $T = 0.20$ J/K is shown in Fig. 2. This figure shows that the interface mobility is a monotonic function of φ in which the [11] and [10] interfaces are limiting cases. The mobility of the [10] interface is as much as ~ 25 times larger than that of the [11] interface at $T = 0.20$ J/K. The orientation dependence of the mobility can be understood through the examination of the microscopic migration mechanism. The interface velocity is determined by the density of kinks and their velocities. While the equilibrium density of kinks on the [11] interface is zero in the limit that $T \to 0$, the [10] interface structure can be viewed as consisting of kinks spaced one lattice spacing apart (see Fig. 1(c)). Therefore, migration of the [11] interface requires the nucleation of double kinks, while no such nucleation event is necessary to move the [10] interface. At high temperature, the two interfaces are thermally roughened to the extent that they contain similar densities of microscopic [10,11] segments and hence move with nearly the same mobility.

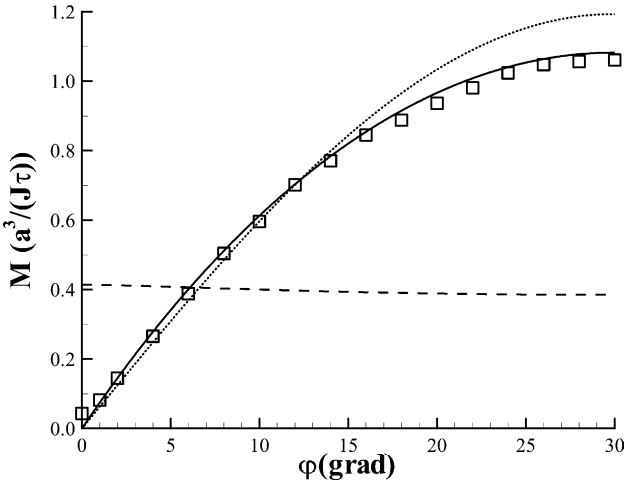

Fig. 2. Orientational dependence of the mobility of the flat interface driven by an external field at $T = 0.20$ J/K. The squares represent the kinetic Monte Carlo simulation. The dashed line represents an analytical solution obtained with an assumption that γ'' is negligible and the reduced mobility is isotropic. The dotted line represents an analytical solution assuming that the reduced mobility is isotropic but using the stiffness rather then interface free energy (Eq. (23)). The solid line represents the analytical solution using the anisotropic reduced mobility and the stiffness (Eq. (25)).

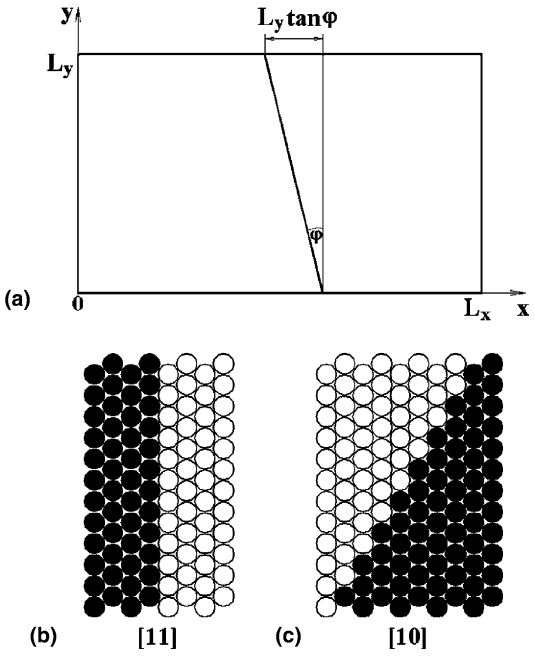

Fig. 1. (a) Schematic illustration of the simulation geometry for a flat interface. Two limiting cases of the flat interface corresponding to two different inclinations: (b) $\varphi = 0$ (labeled [11]) and (c) $\varphi = \pi/6$ (labeled [10]).

Interfaces in the Ising model can also be driven using a capillarity driving force, in which the interface velocity is proportional to the local interface curvature. Additional simulations were performed in which the interface was initially circular. An image of such a shrinking grain is shown in Fig. 3(a). This figure shows that the grain remains roughly circular while shrinking (see also [6]). However, the imposition of an external field of either sign leads to interface profiles that exhibit the 6-fold symmetry of the underlying lattice.

The shape of a shrinking grain in the half-loop geometry was also investigated. Fig. 4 shows the half-loop boundary profile, averaged over 10,000 instantaneous configurations. If the reduced mobility of the boundary

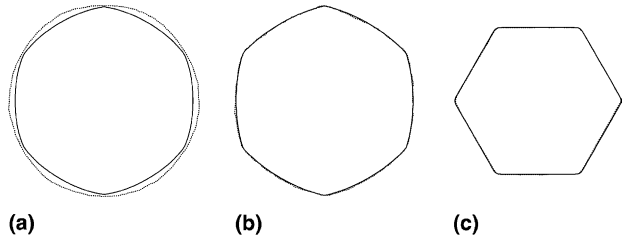

Fig. 3. The grain shape evolution at $T = 0.20$ J/K and (a) $H = 0$, (b) $H = 0.01$ J and (c) $H = -0.01$ J. Solid and dotted lines represent the continuum model and kinetic Monte Carlo (kMC) results, respectively. In all simulations the initial grain shape was a circle with radius of 700 a in the cases (a) and (b) and 500 a in the case (c). The time of evolution in each case was the same for both the kMC and the continuum model. In the case (a), the continuum model was based on Eq. (4) and in the cases (b) and (c), it was based on Eq. (8).

does not depend on boundary orientation, the steady-state half-loop boundary profile (for curvature-driven migration) can be described analytically by [8]

$$y = \frac{w}{\pi} \arccos[e^{-(\pi/w)x}], \tag{6}$$

where the locus of points (x, y) describes the boundary profile (the boundary moves in the x-direction) and w is the half-loop width. The shape obtained from Eq. (6) is also shown in Fig. 4. Examination of this figure demonstrates that in spite of the fact that the boundary mobility is strongly anisotropic; the half-loop is described by the continuum theory with an isotropic reduced mobility.

Taken together, these results present an apparent paradox. The kinetic Monte Carlo simulations show that the interface mobility is strongly anisotropic (at low temperature) and the interface free energy is nearly isotropic (only a 10% variation with inclination at low temperature [6]). These results suggest that the reduced mobility should be strongly anisotropic. On the other hand, the shapes of the half-loop and circular grains shrinking under the sole influence of capillarity are well described assuming that the reduced mobility is isotropic.

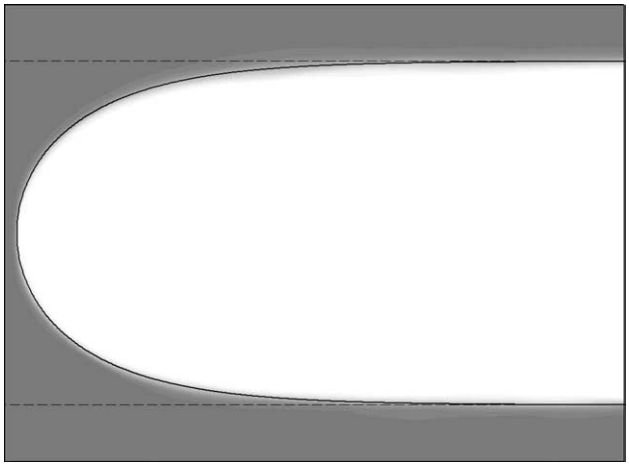

Fig. 4. The average shape of the half-loops determined from simulations at $T = 0.10$ J/K. The intensity of the gray level at each point is proportional to the probability that a spin at this location (relative to the half-loop tip) is equal to −1. The solid lines represent the predicted shape assuming isotropy (Eq. (6)).

3. Sharp interface simulations

We can resolve the apparent paradox raised in the previous section by answering the following questions:

(i) Is the measured interface mobility anisotropy sufficiently large to significantly alter the grain shape in the absence of an external field?

(ii) Is the paradox attributable to the inherent discreteness of the Ising model? In other words, can the kinetic Monte Carlo results (e.g., the combined effects of curvature and external field driven motion) be reproduced in a continuum model?

To address these questions, we compare the Monte Carlo results to those obtained with a sharp-interface model parameterized in terms of the anisotropic mobility found in the kinetic Monte Carlo simulations. The sharp interface equations (Eq. (7) or (8) given below) are solved using a numerical scheme that is especially designed to surface tension driven interface motion [9]. In brief, the interface is parameterized by the position vector $\mathbf{X}(\alpha, t) = (x(\alpha, t), y(\alpha, t))$ where $\alpha = s/L(t)$ is the ratio of the arc length along the interface to the total arc length $L(t)$; α is known as the relative arc length and varies from zero to unity for an arbitrarily shaped interface. The evolution is formulated using the angle $\varphi(\alpha, t)$ between the normal to the interface and a fixed x-axis as basic dynamical variable together with $L(t)$. In this formulation, the curvature is simply $\kappa = L(t)^{-1}\partial\varphi(\alpha, t)/\partial\alpha$ and the evolution equation for $\varphi(\alpha, t)$ has the form of a diffusion equation that is coupled to a separate equation of motion for $L(t)$. This diffusion equation is solved [9] using a pseudo-spectral method where the partial derivatives of $\varphi(\alpha, t)$ with respect to α are calculated in Fourier space, and a semi-implicit scheme is used for time stepping. These ingredients make this scheme extremely accurate and all results reported here are independent of the arc length step $\Delta\alpha$ and time step Δt.

We first investigate the shrinking of a circular grain with no external field. Since γ was found to be nearly isotropic (e.g., $\gamma_{[10]}/\gamma_{[11]} = 1.07$ at $T = 0.20$ J/K [6]), we start from the standard grain growth assumption that $M^* = M\gamma$ (i.e., we neglect γ''), where γ is a constant and M is the function of inclination determined from the kinetic Monte Carlo simulations (e.g., $M_{[10]}/M_{[11]} \approx 25$ at $T = 0.20$ J/K). Fig. 3(a) shows interface profiles from both the sharp interface and Monte Carlo simulations at the same simulation time. At the time at which these profiles were recorded, the rate of change of the grain

area was independent of time. While the interface profile obtained from the Monte Carlo simulation is circular, the interface profile predicted by the sharp interface model has a pronounced 6-fold symmetry – the same as the symmetry of $M(\varphi)$ extracted from the triangular lattice Ising model. The discrepancy between the Monte Carlo and sharp interface model results demonstrates that either the widely used [8] equation of motion for capillarity driven grain boundaries (Eq. (4)) is invalid or the discreteness of the Ising model is essential.

To exclude the possibility that the discreteness of the Ising models is essential, we look for a continuum model that is capable of reproducing the kinetic Monte Carlo simulation results. The Monte Carlo simulation results themselves suggest an appropriate continuum model. Since an initially circular grains shrinks isotropically (i.e., as a circle), we can describe the shape evolution as

$$v = M^*\kappa, \tag{7}$$

where M^* is isotropic (independent of φ) and can be extracted directly from the Monte Carlo simulations, $M^* = (\mathrm{d}A/\mathrm{d}t)_{\mathrm{MC}}/2\pi$, where $(\mathrm{d}A/\mathrm{d}t)_{\mathrm{MC}}$ is the rate of change of the grain area). This will also predict the appropriate half-loop shape evolution (which was shown, in the previous section, to be consistent with an isotropic reduced mobility). Since this expression only describes capillarity driven motion, it must be extended to also include the effects of an external field. Hence, we write

$$v = -M^*\kappa + M(\varphi)P_{\mathrm{e}}, \tag{8}$$

where P_{e} is the driving force associated with the external field. Fig. 3(b) and (c) compare the grain shapes predicted by the sharp interface model and those from the kinetic Monte Carlo simulations for different signs of the external driving force P_{e}. These figures clearly demonstrate that the discrete Monte Carlo results can be accurately reproduced with the continuum, sharp interface model and Eq. (8). This answers the second question raised at the beginning of this section.

The calculations performed with the continuum, sharp interface model above demonstrate that the reduced mobility in the triangular lattice is isotropic (or, at least, only weakly anisotropic). However, the kinetic Monte Carlo certainly demonstrates that the mobility is strongly anisotropic while the interface free energy (in the case of triangle lattice case studied here) is nearly isotropic. Clearly, the strong anisotropy of the mobility cannot be canceled by the weak anisotropy of the interface free energy. This conclusively demonstrates that the reduced mobility is not the product of the interface mobility and free energy, i.e., M^* is not equal to $M\gamma$. One possible interpretation of this conclusion is that neglecting the γ'' in the equation of motion (Eq. (3)) is inappropriate, i.e., $M^* = M(\gamma + \gamma'')$, where $(\gamma + \gamma'')$ is the interface stiffness. Since M^* is nearly isotropic and M is strongly anisotropic, $(\gamma + \gamma'')$ must also be strongly anisotropic (i.e., much more anisotropic than γ itself). In order to investigate this assertion, we must independently determine the interface stiffness.

4. Analytical prediction of the interface stiffness

We now derive an expression for the stiffness of an interface in the triangular lattice Ising model. Consider a segment of a flat boundary of length L and inclination angle φ. The geometrically necessary number of kinks on this segment is

$$K = \frac{L}{a\sqrt{3}/2}\sin\varphi, \tag{9}$$

where $a\sqrt{3}/2$ is the kink height. Note that there may be additional, thermally generated kinks of equal numbers of both signs. The number of such kinks decreases with decreasing temperature (as per an Arrhenius relation) and they are neglected in the present analysis. The total number of lattice sites between the geometrically necessary kinks is

$$N = N_{\varphi=0} - \frac{1}{2}K = \frac{L}{a}\cos\varphi - \frac{1}{2}K, \tag{10}$$

where $N_{\varphi=0}$ is the number of sites along the projection of the segment onto the [11] direction.

If $\varphi = 0$, the interface energy per site is $2J$. For $\varphi \neq 0$, the interface energy increases by J per kink. Therefore, the segment of length L has energy

$$L\gamma_E = N_{\varphi=0}\cdot 2J + K\cdot J = \frac{2JL}{a}\left(\cos\varphi + \frac{1}{\sqrt{3}}\sin\varphi\right). \tag{11}$$

This equation shows that the contribution of the internal energy of the interface to the stiffness at $T = 0$ is

$$\gamma_E + \gamma''_E = 0. \tag{12}$$

Note, however, that this expression is inapplicable at $\varphi = n\pi/3$ (n is integer) in a triangular lattice, where the stiffness is singular. Also note that this expression is accurate at low temperatures, where the density of thermally nucleated kink pairs is small. These results suggest that the behavior of the interface stiffness is dominated by the interface entropy.

The configuration entropy of this segment can be determined from the number of ways there are to arrange K kinks and N non-kink sites using Stirling's approximation

$$\begin{aligned} S_\gamma &= k_{\mathrm{B}}\ln\frac{(N+K)!}{N!K!} \\ &= -\frac{k_{\mathrm{B}}L}{a}\left[\left(\frac{2\sin\varphi}{\sqrt{3}}\right)\ln\left(\frac{2\sin\varphi}{\sqrt{3}\cos\varphi+\sin\varphi}\right)\right. \\ &\quad \left. + \left(\frac{\sqrt{3}\cos\varphi-\sin\varphi}{\sqrt{3}}\right)\ln\left(\frac{\sqrt{3}\cos\varphi-\sin\varphi}{\sqrt{3}\cos\varphi+\sin\varphi}\right)\right]. \end{aligned} \tag{13}$$

Combining Eqs. (12) and (13), we can write the interface stiffness as a function of interface orientation and temperature as

$$\gamma + \gamma'' = -T(S_\gamma + S''_\gamma) = \frac{2\sqrt{3}k_B T}{a\sin(3\varphi)}. \tag{14}$$

As expected, the stiffness is strongly anisotropic.

5. Analytical prediction of the interface mobility

We now address the question of "does the interface stiffness anisotropy compensate for the anisotropy in the interface mobility such that the reduced mobility is nearly isotropic (in the triangular lattice Ising model)?" We begin this discussion by focusing on the simple case of a small inclination angle, φ, and a small external field ($H \ll k_B T$). Consider the kink geometry shown in Fig. 5. At each Monte Carlo step every atomic site is sampled, on average, one time. At low temperature, only the spins at sites 1 and 2 can flip (at any appreciable rate). When site 1 is sampled, the spin flip is accepted with unit probability $P_1 = 1$ while the flip of spin 2 is accepted with probability $P_2 = e^{-2H/k_B T}$. The kink drift velocity is then

$$v_k = \frac{a}{\tau}(P_1 - P_2) = \frac{a}{\tau}(1 - e^{-2H/k_B T}) \approx \frac{a}{\tau}\frac{2}{k_B T}H. \tag{15}$$

We neglected the possibilities that a particular site may be sampled more than once during a single Monte Carlo step or that a kink may move by more than single lattice spacing in one Monte Carlo step. Such corrections are of order $(H/k_B T)^2$ and hence negligible in the limit $H \ll k_B T$.

When the kinks move by the average inter-kink separation ($d_k = \sqrt{3}a/2\tan\varphi$), the interface moves by the projection of the kink height onto the interface normal ($d_i = \sqrt{3}a/2\cos\varphi$). Therefore, the net interface velocity is

$$v = \frac{d_i}{d_k} v_k \approx \frac{a}{\tau}\frac{2\varphi}{k_B T}H. \tag{16}$$

Since the external driving force in the triangular lattice Ising model is $P = 4H/(\sqrt{3}a^2)$, the interface mobility at small inclination is

$$M = \frac{\sqrt{3}a^3}{2\tau}\frac{\varphi}{k_B T}. \tag{17}$$

This expression shows that the interface mobility scales linearly with the inclination angle and is zero at $\varphi = 0$ (i.e., the interface [11]). Recall, however, that the kinetic Monte Carlo simulations show that the interface mobility is small but finite at low temperature for the [11] interface. This discrepancy is due to the fact that we neglected the thermal generation of kinks.

In the small inclination limit, the interface stiffness (Eq. 15) reduces to

$$\gamma + \gamma'' = -T(S_\gamma + S''_\gamma) = \frac{2}{\sqrt{3}a}\frac{k_B T}{\varphi}. \tag{18}$$

Therefore, the reduced mobility, $M^* = M(\gamma + \gamma'')$, can be found from Eqs. (17) and (18) to be

$$M^* = \frac{a^2}{\tau}. \tag{19}$$

Clearly, although the mobility and the interface stiffness are strongly anisotropic, the reduced mobility in the small inclination angle limit is independent of inclination in the triangular lattice Ising model.

We can test this conclusion over the entire range of inclinations. To do this, we assume that the reduced mobility is isotropic (as suggested above based upon the small angle analytical derivation and the analysis of the kinetic Monte Carlo results using the continuum sharp interface model). Applying this assumption to the case of the shrinking initially circular grain gives us a relationship between the rate of change of grain area and the reduced mobility:

$$\frac{dA}{dt} = -\oint vR\,d\varphi = -\oint M^*\kappa R\,d\varphi = -M^*\oint d\varphi = -2\pi M^* \tag{20}$$

Combining this result with the definition of the reduced mobility shows

$$M = -\frac{1}{2\pi(\gamma + \gamma'')}\frac{dA}{dt}. \tag{21}$$

To apply Eq. (21), we require an expression for dA/dt. Such an expression was obtained in [10] for low temperature. This derivation is based upon the observation that at low temperature, the net number of kinks (i.e., the number of + kinks minus the number of − kinks) is exactly six for any closed shape on a triangular lattice as illustrated in Fig. 6. Any of the spins at kink sites can flip with no increase in the system energy, such that the rate of such flips is $1/\tau$. The area per spin in the triangular lattice is $a^2\sqrt{3}/2$. Therefore,

$$\frac{dA}{dt} = -3\sqrt{3}\frac{a^2}{\tau}. \tag{22}$$

Combining Eqs. (21), (14) and (22) we find

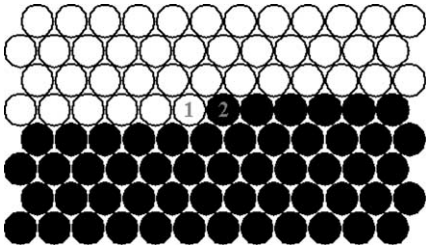

Fig. 5. Illustration of a kink in an [11] interface on a triangular lattice. Spins labeled by 1 and 2 are the only ones that can flip in the zero temperature limit.

$$M = \frac{3a^3}{4\pi\tau}\frac{1}{k_B T}\sin(3\varphi). \quad (23)$$

Fig. 2 shows a comparison of the mobility calculated using Eq. (23) with the kinetic Monte Carlo simulation data obtained from the flat interface simulations. This comparison suggests that the assumption that the reduced mobility is isotropic (i.e., the main assumption in deriving Eq. (15)) is rather good. Therefore, the anisotropy of the interface mobility is almost completely compensated by the anisotropy in the interface stiffness in the triangular lattice Ising model. On the other hand, if we employ the widely used assumption that the reduced mobility is simply $M\gamma$ rather than $M(\gamma+\gamma'')$, we would be forced to conclude that the interface mobility is nearly isotropic – in strong disagreement with the kinetic Monte Carlo results (see Fig. 2). This clearly demonstrates the importance of using interface stiffness rather than the interface free energy in the analysis of the capillarity driving interface migration.

Fig. 2 suggests that the reduced mobility is not precisely isotropic. A more rigorous derivation of the reduced mobility on a triangular lattice [11] yields

$$M^* = \frac{a^2}{\tau}\frac{1}{(\cos\varphi + \frac{1}{\sqrt{3}}\sin\varphi)}. \quad (24)$$

Combining Eq. (24) above with the expression for the interface stiffness, we obtain

$$M = \frac{\sqrt{3}a^3}{2\tau}\frac{1}{k_B T}\frac{\sin\varphi(\cos\varphi - \frac{1}{\sqrt{3}}\sin\varphi)}{(\cos\varphi + \frac{1}{\sqrt{3}}\sin\varphi)}. \quad (25)$$

This expression, also plotted in Fig. 2, is in an even better agreement with the kinetic Monte Carlo results than Eq. (23). The remaining discrepancies are attributable to neglecting thermal kinks in the analysis. We note that for the square lattice analytical expressions for the mobility [12,13] and the reduced mobility [14] where derived previously. Interestingly, in this case, the shape of a shrinking grain is markedly less isotropic owing to the fact that the reduced mobility is more anisotropic for the square lattice.

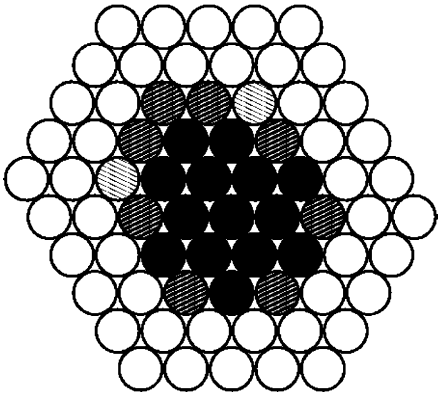

Fig. 6. Illustration of a grain on a triangular lattice showing shaded boundary spins that flip with no change of total energy, and hence are the only spins that can flip in the zero temperature limit. We can show that, in this limit, the number of shaded spins inside the grain (8 in the example above) minus the number of the shaded spins outside the grain (2 in. the example above) is equal to six in general.

6. Discussion and concluding remarks

In this work, we have examined interface motion under different driving forces in the Ising model at low temperature. The starting point of our investigation was the puzzling observation from simulations that a circular grain shrinks as a nearly perfect circle on a triangular lattice under the action of capillarity alone, while the same grain shrinks or expands with the lattice anisotropy (i.e., as a near hexagon) when an external field is switched on. The latter is easily explained by the fact that interface facets are nearly immobile at low temperature, due to the rarity of kink nucleation, while interfaces with a high density of geometrically necessary kinks are highly mobile. As a result, the interface mobility is strongly anisotropic and the grain shape reflects the underlying anisotropy of the lattice under the action of an external field. More puzzling was the observation that interface motion driven by curvature can be quasi-isotropic, in apparent contradiction with the fact that the interface mobility is highly anisotropic.

We have obtained excellent agreement between the Monte Carlo simulations results and a sharp-interface model where the reduced mobility for curvature-driven motion is isotropic and the mobility for field-driven motion is highly anisotropic. Based on this agreement, one might naively be tempted to conclude that the interface mobility depends on the nature of the driving force. We have learned that this is incorrect because a quasi-isotropic *reduced* mobility does not imply a quasi-isotropic interface mobility. This is more subtle than we initially expected and can be explained on the basis of two observations. First, the correct expression for the reduced mobility given by the Herring relation is the product of the bare mobility (which is itself anisotropic, as discussed above) and the interface stiffness $\gamma+\gamma''$. The interface stiffness is also highly anisotropic *if* one includes the entropic part of γ, TS_γ. Second, the anisotropies of the stiffness and of the mobility almost cancel each other to produce a nearly isotropic reduced mobility. This cancellation occurs because the entropic part of the stiffness TS''_γ is large for inclinations where the mobility is low and vice versa. This, in turn, occurs because the number of geometrically necessary kinks, and hence the kink configurational entropy S_γ, increases rapidly when the inclination is varied near a singular

orientation. In contrast, this entropy has only a weak dependence on inclination near mobile interfaces with a high density of kinks.

Our results show that a reliable comparison of the mobilities obtained from experiments, where the same boundary moves subject to both an external driving force (elastic or magnetic field) and capillarity, requires a precise knowledge of the boundary stiffness rather than simply the boundary free energy. The term γ'', which is usually neglected in most theories of grain boundary migration, cannot a prioiri be neglected. Unfortunately, we do not know of any experiment or simulation to date where this term was determined reliably.

We expect the main conclusion that the mobility is independent of driving force to remain true for grain boundaries in polycrystalline materials. Less certain, however, is whether the error introduced by neglecting γ'' in the reduced mobility is as dramatic for these boundaries as it is for the idealized interfaces studied here in the Ising model. Clearly, grain boundaries in real materials have complex atomic structure and defects contained within grain boundaries interact elastically. Consequently, the fact that the enthalpic part of the stiffness vanishes exactly in the Ising model, where γ_E is simply the local bond cutting energy, is an over-simplification. Recent molecular dynamic simulations for the U-shape grain geometry (analogous to Fig. 5) for the Lennard–Jones system has shown that the shape of the grain is consistent with a reduced mobility that is nearly isotropic [15]. Therefore, we expect the basic rule that the "stiffness is high where the mobility is low (and vice versa)" to remain valid for real grain boundaries. Extensive molecular dynamics simulations are presently underway to test the validity of this rule for these boundaries and experiments. Work is also in progress to extend the methods of this article to the three-dimensional (3D) Ising model [11].

Acknowledgements

This research was supported by the U.S. Department of Energy, Office of Basic Energy Sciences, Materials Science Division, under contract numbers DE-FG02-92ER45471 (AEL and AK) and DE-FG02-99ER45797 (MIM, MH, DJS), as well as additional financial support through the DOE Computational Materials Science Network Program. This research also benefited from allocation of computer time at the Northeastern University Advanced Scientific Computing Center.

References

[1] Hillert M. Scr Metall 1983;17:237.
[2] Winning M, Gottstein G, Shvindlerman LS. Acta Mater 2002;50:353.
[3] Molodov DA, Gottstein G, Heringhaus F, Shvindlerman LS. Mater Sci Forum 1999;294:127.
[4] Herring C. Surface tension as a motivation for sintering. In: Gomer R et al., editors. The physics of powder metallurgy. New York (NY): McGraw-Hill; 1949.
[5] Boettinger WJ, Coriell SR, Greer AL, Karma A, Kurz W, Rappaz M, Trivedi R. Acta Mater 2000;48:43–70.
[6] Mendelev MI, Srolovitz DJ, Gottstein G, Shvindlerman LS. J Mater Res 2002;17:234.
[7] Binder K. Monte Carlo simulation in statistical physics. Berlin: Springer-Verlag; 1979. p. 376.
[8] Gottstein G, Shvindlerman LS. Grain interface migration in metals: thermo-dynamics, kinetics, applications. Boca Raton (FL): CRC Press; 1999. p. 203.
[9] Hou TY, Lowengrub JS, Shelley M. J Comput Phys 1994;114:312–38.
[10] Kandel D, Domany E. J Statist Phys 1990;58:685.
[11] Lobkovsky AE, Karma A. Private communication.
[12] Barma M. J Phys A 1992;25:L693.
[13] Rikvold PA, Kolesik M. J Statist Phys 2000;100:377.
[14] Spohn H. J Statist Phys 1993;71:1081.
[15] Upmanyu M, Hassold GN, Kazaryan A, Holm EA, Wang Y, Patton B, Srolovitz DJ. Interf Sci 2002;10:201.